



Narrow-band ultra-low-frequency wave observations by MESSENGER during its January 2008 flyby through Mercury's magnetosphere

Scott A. Boardsen,^{1,2} Brian J. Anderson,³ Mario H. Acuña,² James A. Slavin,²
Haje Korth,³ and Sean C. Solomon⁴

Received 16 September 2008; revised 31 October 2008; accepted 5 November 2008; published 3 January 2009.

[1] During MESSENGER's first flyby of Mercury, numerous narrow-band ultra-low-frequency (ULF) waves and their harmonics were detected between closest approach (CA) and the outbound magnetopause (MP) crossing. The fundamental mode was at frequencies between the He⁺ (f_{cHe^+}) and the H⁺ (f_{cH^+}) cyclotron frequencies. A boundary layer (BL) was detected before the MP crossing. The ULF frequency and amplitude increased from CA to the edge of the BL. In the BL the frequency dropped by a factor of 2, and the amplitude increased by an order of magnitude. There was a large variation in the wave-normal angle (Ψ), with a slight tendency for Ψ to be perpendicular to the ambient magnetic field near CA and parallel away from CA. Near CA the parallel power tended to be larger than the perpendicular power, while away from CA the perpendicular power dominated. Large variations in wave polarization properties were observed. **Citation:** Boardsen, S. A., B. J. Anderson, M. H. Acuña, J. A. Slavin, H. Korth, and S. C. Solomon (2009), Narrow-band ultra-low-frequency wave observations by MESSENGER during its January 2008 flyby through Mercury's magnetosphere, *Geophys. Res. Lett.*, 36, L01104, doi:10.1029/2008GL036034.

1. Introduction

[2] During the first flyby of Mercury by the Mercury Surface, Space ENvironment, GEochemistry, and Ranging (MESSENGER) spacecraft on 14 January 2008, bursts of narrow-band ultra-low-frequency (ULF) waves were detected by the Magnetometer almost continuously from the closest approach (CA) to the outbound magnetopause (MP) crossing [Slavin *et al.*, 2008]. During the first Mariner 10 flyby of Mercury on 29 March 1974, a ~38-s burst of narrow-band ULF waves was detected at 1.34 R_M (where R_M is Mercury's radius) at low Mercury solar orbital (MSO) latitudes just inbound of CA [Russell, 1989]. The frequency of these emissions was ~0.5 Hz, or ~40% of the H⁺ cyclotron frequency (f_{cH^+}), which was ~1.31 Hz. Russell noted that this ULF wave burst had a strong linear polarization close to the meridian plane. The maximum peak-to-

peak amplitude transverse to the ambient field was ~4 nT, and the maximum peak-to-peak compressional amplitude was ~1.5 nT. Russell [1989] suggested that these waves might be field line resonances (FLRs), but he noted that they did not have a strong azimuthal component or exhibit harmonics that are typical of terrestrial FLRs [Takahashi *et al.*, 1984]. If these waves were present during the outbound trajectory of Mariner 10, they were masked by strong substorm activity [Siscoe *et al.*, 1975]. No such waves were reported during Mariner 10's third encounter.

[3] ULF waves in this frequency range and their mode coupling will be strongly modified by cyclotron resonances of both heavy [Othmer *et al.*, 1999; Glassmeier *et al.*, 2003; Kim *et al.*, 2008] and light [Kim and Lee, 2003] ion species. For plasma composed of protons and Na⁺, Othmer *et al.* [1999] showed that the crossover frequency where the polarization reverses is the point where compressional wave energy is most likely to convert into FLRs. By assuming that the ULF frequency given by Russell [1989] is at this crossover frequency, these authors placed a lower limit of ~14% on the fractional composition of Na⁺. Numerous heavy ion species were detected by MESSENGER's Fast Imaging Plasma Spectrometer (FIPS) during the probe's first flyby, with Na⁺ being the most abundant [Zurbuchen *et al.*, 2008] of the heavy ions.

[4] Glassmeier *et al.* [2004] pointed out that the magnetopause of Mercury is very stiff compared with that of the gas giant planets and even that of Earth, so the buffeting of Mercury's magnetosphere by the solar wind should produce a constant ringing in Mercury's magnetosphere, creating small-amplitude compressional ULF waves that can be partially absorbed at resonances. Kim and Lee [2003] simulated wave generation in Mercury's magnetosphere by inputting a pulse of energy from the magnetopause end of a box-model magnetosphere consisting of a cold H⁺ plasma. They found that waves were excited at the perpendicular ion cyclotron resonance (PICR) frequency, ~0.67 f_{cH^+} , along with the fundamental magnetohydrodynamic (MHD) field line resonance, which occurred at much lower frequencies. The wave energy at the resonance near f_{cH^+} is a combination of both right- and left-handed polarizations, with a slight bias in the right-handed direction. Kim *et al.* [2008] extended their simulation to include Na⁺ and found that the coupling frequency was at the ion-ion hybrid resonance frequency. Furthermore they found no evidence of FLR excitation at the crossover frequency predicted by Othmer *et al.* [1999]. In the Kim and Lee [2003] simulation, the plasma density varied with all other ambient plasma parameters fixed, while in the Kim *et al.* [2008] simulation

¹Goddard Earth Sciences and Technology Center, University of Maryland, Baltimore County, Baltimore, Maryland, USA.

²NASA Goddard Space Flight Center, Greenbelt, Maryland, USA.

³Johns Hopkins University Applied Physics Laboratory, Laurel, Maryland, USA.

⁴Department of Terrestrial Magnetism, Carnegie Institution of Washington, Washington, D. C., USA.

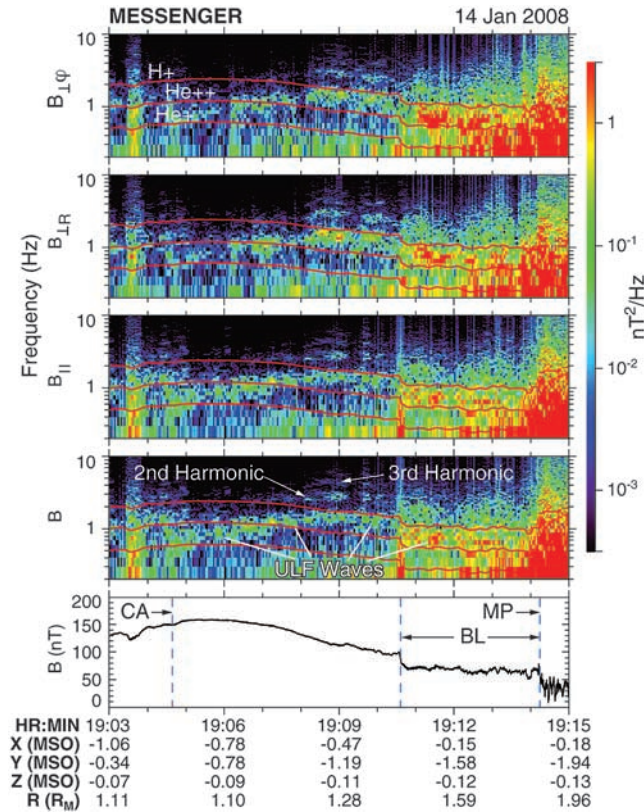


Figure 1. Dynamic spectrograms from MESSENGER's first flyby of Mercury. The red curves show the H^+ , He^{++} , and He^+ cyclotron frequencies.

the ratio of H^+ to Na^+ varied across the simulation box with other parameters fixed.

[5] According to *Glassmeier et al.* [2004], the FLRs at Mercury are likely to be composed of kinetic Alfvén waves. These authors predict that such kinetic Alfvén waves will create field-aligned potential drops of ~ 0.5 keV, and electrons should subsequently be heated by these waves. MESSENGER indirectly detected ~ 1 -keV electrons near the time that the ULF wave activity began [*Slavin et al.*, 2008].

[6] In addition to being an important source of energy transfer within Mercury's magnetosphere, the ULF waves found by MESSENGER could play an important diagnostic role. If the ion-ion resonance frequencies can be identified, then the ion composition of the plasma can be estimated [*Kim et al.*, 2008]. It will be difficult to resolve frequencies significantly below f_{CH^+} during MESSENGER's flybys of Mercury, but detections of all the resonances might be possible during the orbital phase of the mission [*Boardsen and Slavin*, 2007].

[7] The purpose of this paper is to expand on the investigation of these waves beyond what was reported by *Slavin et al.* [2008]. In particular we determine the intensity and spatial extent of these emissions, using dynamic spectrograms of the magnetic field measured during the flyby. We characterize the wave properties and compare them against the Mariner 10 results and theoretical models.

2. Observations

[8] During MESSENGER's first flyby of Mercury, the Magnetometer sampled Mercury's magnetic field 20 times

per second [*Anderson et al.*, 2008]. Mercury's magnetosphere was quiet during the flyby, and no substorms were detected. The lack of substorm activity, thought to be the result of the northward MSO B_z component of the interplanetary magnetic field [*Slavin et al.*, 2008], makes it easier to detect these narrow-band ULF waves. On the inbound leg, from the MP crossing at 18:43:02 UT to 19:02:20 UT (~ 2 minutes before CA), narrow-band ULF wave activity was weak. During this 19-minute interval only four brief ULF bursts, whose durations varied from 2 to 6 s, were identified. The frequencies of these bursts ranged between ~ 3 and $\sim 10 f_{CH^+}$, and their peak-to-peak amplitudes varied between 0.3 and 0.5 nT. The last inbound event was observed at $\sim 18:55:10$ UT, and its frequency was $\sim 3.1 f_{CH^+}$. In contrast, an abundance of narrow-band ULF waves was detected during the outbound leg between 19:02:20 UT and the outbound MP crossing at 19:14:15 UT. We focus on these outbound observations.

[9] A dynamic spectrogram of the field during MESSENGER's flyby of Mercury, covering the period of high ULF-wave activity, is shown in Figure 1. This dynamic spectrogram was created from individual fast Fourier transform (FFT) spectra generated over 8-s intervals, stepping 4 s in time from one spectrum to the next. For each spectrum, the data have been linearly de-trended and rotated into coordinates perpendicular (\perp_ϕ , \perp_R) and parallel (\parallel) to the local magnetic field. The perpendicular component (\perp_ϕ) points along the projection of the azimuthal direction into the perpendicular plane. The H^+ , He^{++} , and He^+ cyclotron frequencies are indicated in Figure 1. For context, the magnetic field magnitude is displayed on the bottom panel. The CA at 19:04:39 UT, the outbound boundary layer (BL) starting at 19:10:37 UT, and the outbound MP crossing are indicated. The step-like ~ 20 -nT decrease in magnetic field magnitude marks the start of this BL. Two possible explanations for this BL have been proposed [*Slavin et al.*, 2008].

[10] Examination of Figure 1 between CA and the outbound MP crossing shows that the first-appearing narrow-band ULF waves were at frequencies just above the He^+ cyclotron frequency (f_{cHe^+}). There was a systematic increase in frequency to just below the H^+ frequency (f_{cH^+}) before the spacecraft crossed into the BL. Upon crossing into the BL, there was an associated downward step in ULF frequency that tracked the downward step in magnetic field magnitude accompanied by an increase in ULF wave amplitude.

[11] Around 19:09 UT, harmonics of these ULF waves are clearly visible. At that time the fundamental component of the ULF waves was propagating within 30° of the background magnetic field direction, while the second harmonic was propagating within 30° of the plane perpendicular to the background magnetic field. The ratios of the first to the second, third, and fourth harmonics are 2.1 ± 0.5 , 3.3 ± 0.5 , and 4.3 ± 0.6 , respectively. Once in orbit, because of its lower orbital speed relative to its flyby speed, MESSENGER will be able to resolve these harmonics to higher resolution.

[12] Between 19:02:20 UT and the outbound MP crossing, thirty-six ULF wave intervals were identified by visual inspection of the MESSENGER Magnetometer time series data. Time series and hodograms for two examples are shown in Figures 2a and 2b and Figures 2c and 2d,

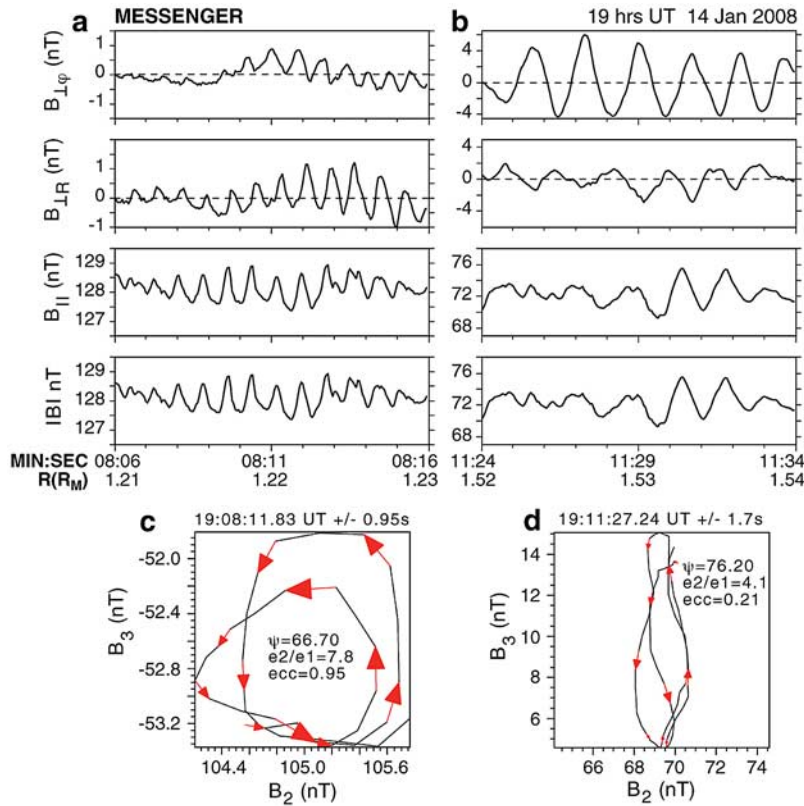


Figure 2. (a) Time-series examples of ULF waves detected outbound from closest approach. (b) Example ULF waves in the BL. Hodograms of the time series shown in Figures (c) 2a and (d) 2b. Axes B_2 and B_3 are the directions of intermediate and maximum variance, respectively. The wave-normal angle, ratio of median to minimum eigenvalue, and ellipticity are given for each hodogram.

respectively. The hodogram axes B_2 and B_3 correspond to the directions of intermediate and maximum variance, respectively. The direction of minimum variance (the B_1 axis) was chosen such that its dot product with the direction of the ambient magnetic field is positive. The arrowheads on the hodograms indicate the direction of time. At the start of the interval shown in Figure 2a, the parallel magnetic field component (whose oscillations are non-sinusoidal) dominates the perpendicular components, and at the end the perpendicular components dominate the parallel component. The maximum peak-to-peak amplitude is about 2 nT. A hodogram for ~ 2 cycles is shown in Figure 2c; the wave-normal angle is $\sim 66^\circ$, and its ellipticity (~ 0.95) indicates strongly circularly polarized waves rotating in the right-handed direction about the magnetic field. Figure 2d shows an example of the time series in the BL, where the component $B_{\perp\phi}$ lies close to the azimuthal direction and its maximum peak-to-peak amplitude is ~ 10 nT. The dominance of the azimuthal component is consistent with terrestrial observations of narrow-band ULF waves in geosynchronous orbit [Takahashi *et al.*, 1984]. The parallel component has maximum peak-to-peak amplitudes of ~ 4 nT for this event. Figure 2d shows a hodogram for a portion of the time series in Figure 2b; the wave-normal angle is $\sim 76^\circ$, and its ellipticity (~ 0.21) is in the right-handed direction.

[13] Wave polarization parameters were computed for these ULF intervals using the method of Arthur *et al.* [1976]. The selected intervals typically ranged from 4 to

8 s in duration. Figure 3 shows the results of this analysis. Of the 36 intervals, the degree of polarization (coherency), the ratio of coherent wave power to the total wave power, was less than 0.5 for four intervals. These four intervals are not used. The median degree of polarization of the remaining 32 intervals was 0.84. The top panel displays the frequency of the ULF wave packets during the encounter. The solid lines are located at f_{cH^+} , $f_{cHe^{++}}$, and f_{cHe^+} . Note that the majority of these packets are observed outbound from CA. Except for a packet at 19:02 UT (not shown), all packets show frequencies between f_{cHe^+} and f_{cH^+} . The frequency of the packet at 19:02 was $\sim 0.16 f_{cH^+}$. As noted earlier, there is a systematic increase in frequency from closest approach to the step transition at around 19:10 UT.

[14] The second panel displays the ellipticity (ratio of minor to major axis) of the polarization ellipse. Positive (negative) ellipticity indicates right- (left-) handed polarization with respect to the ambient magnetic field. Of the 32 events, 26 were found to have right-handed polarization. The observed right-handed dominance of these waves is consistent with models of Kim and Lee [2003] that showed a weak steady-state dominance of right-handed waves. The third panel displays the wave-normal angle (Ψ), the angle between the ambient magnetic field and the wave vector. Note that the majority of these waves are oblique to the background field. Of the 32 events, 20 have wave-normal angles greater than 45° . The error estimates for Ψ were derived from the ratio of the minimum to the intermediate

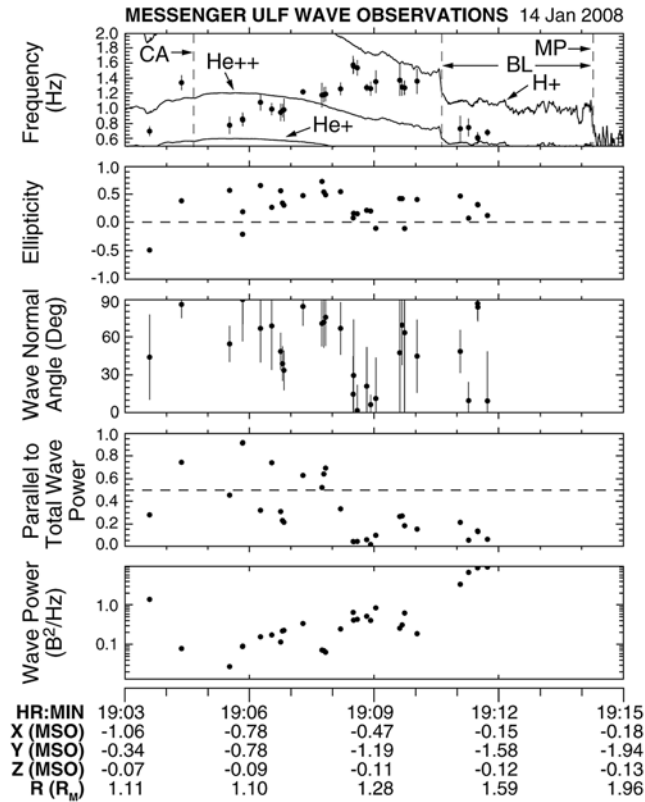


Figure 3. Polarization parameters of ULF waves observed during MESSENGER's first flyby of Mercury.

eigenvalues and the number of frequencies (5) used to compute the coherency matrix [Khrabrov and Sonnerup, 1998]. There is a slight tendency for Ψ to be more perpendicular to the ambient magnetic field near CA and parallel to the ambient magnetic field away from CA. The fourth panel shows the ratio of the power parallel to the magnetic field to the total power. The parallel power is dominant in 10 of the 32 events. Near CA the parallel power tended to dominate, while away from CA the perpendicular power tended to dominate. The fifth panel is the total wave power. The power in these ULF oscillations steadily increased outbound from CA, with an increase by an order of magnitude across the boundary at 19:10 UT.

3. Discussion

[15] The major finding of this study is the observation of narrow-band ULF waves whose frequency systematically increased outbound from CA, with frequencies starting just above f_{cHe^+} near CA and rising to just below f_{cH^+} near the start of the BL; in the BL the frequencies drop. The wave power in these emissions also increased outbound, and jumped by a factor of 10 in the BL. The reason for this variation in frequency and power is not clear. For example, if the plasma is H^+ dominated [Kim and Lee, 2003] then these frequencies could be generated by PICR; a sharp decrease in plasma density with increasing altitude, followed by an increase in density across the boundary layer, would be required to create the observed frequency variation.

[16] If multiple ion species make up the plasma, the frequency could be determined by either ion-ion resonances [Kim *et al.*, 2008] or the cross-over frequency [Othmer *et al.*, 1999]. Zurbuchen *et al.* [2008] detected many ion signatures, including significant contributions from He^+ , He^{++} , and O^+ among the light ions and Na^+ and Mg^+ among the heavy ions; the relative contributions between H^+ and these heavier ion species have not been determined. The observed frequency and amplitude (Figure 3) seem to vary smoothly across the $f_{cHe^{++}}$ boundary, suggesting that the ions heavier than H^+ are just trace particles and don't make a significant contribution to the plasma in the region where these waves are detected.

[17] The observations show that the magnitude of $B_{||}$ is frequently on the order of that of B_{\perp} , which is not consistent with the FLR interpretation [Kim *et al.*, 2008]. Kim *et al.* [2008] suggested that the presence of a significant $B_{||}$ component is more consistent with a cavity mode. If so, the observed drift in frequencies could be related to a yet to be determined drift in a cavity frequency. If cavity frequencies vary as the size of the magnetosphere, we would infer that the magnetosphere contracted over the time period from CA to the edge of the BL, and a sudden expansion followed. More realistic magnetosphere models will be required to determine these cavity frequencies and how they should drift as the shape of the magnetosphere changes.

[18] Instead of these waves being associated with FLRs or cavity modes they could be related to local plasma instabilities at the magnetic equator. The planetary loss cone angle at 1.08 and 1.4 R_M is 70° and 40° , respectively, and the resulting ion distributions should be highly unstable to the generation of waves. The red dots in Figures 4a and 4b show where these waves were detected during the MESSENGER and Mariner 10 flybys. This sparse sampling suggests that these waves may be primarily confined to near

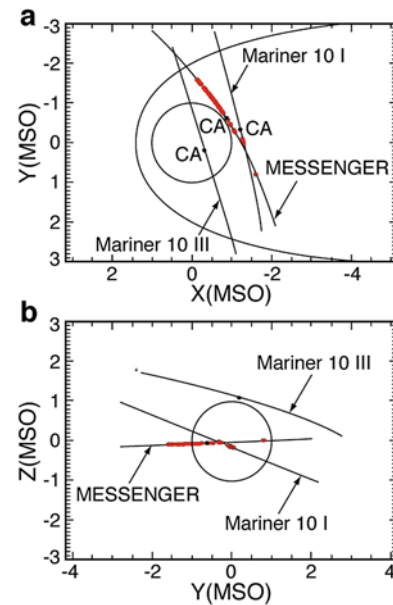


Figure 4. (a) X-Y and (b) Y-Z projections of the three Mercury flybys. The red dots indicate where these narrow-band ULF waves were detected. Note their proximity to the equator.

the magnetic equator (where the loss cone anisotropy is largest), which would indicate that they are not FLRs. The second and third MESSENGER flybys will also be along the equator, and the latitudinal distribution of these waves will not be resolved until MESSENGER is in its near-polar orbit about Mercury in 2011.

4. Conclusion

[19] During MESSENGER's first Mercury flyby, numerous narrow-band ULF waves and their harmonics were detected between CA and the outbound MP crossing. The fundamental mode was at frequencies between f_{cHe^+} and the f_{cH^+} . A BL was detected a few minutes before the outbound magnetopause crossing [Slavin *et al.*, 2008]. The frequency and amplitude both increased from CA to the start of the BL. In this BL there was a decrease in ULF frequency and an increase in wave power. MESSENGER detected a large variation in the wave polarization properties. The majority of these waves with ellipticity magnitudes greater than 0.25 were right-hand polarized. Near CA the parallel power tended to be larger than the perpendicular power, while away from CA the perpendicular power dominated. There was a large variation in Ψ , with a slight tendency for Ψ to be perpendicular to the ambient magnetic field near CA and parallel away from CA.

[20] **Acknowledgments.** The MESSENGER project is supported by the NASA Discovery Program under contracts NAS5-97271 to the Johns Hopkins University Applied Physics Laboratory and NASW-00002 to the Carnegie Institution of Washington.

References

- Anderson, B. J., M. H. Acuña, H. Korth, M. E. Purucker, C. L. Johnson, J. A. Slavin, S. C. Solomon, and R. L. McNutt Jr. (2008), The structure of Mercury's magnetic field from MESSENGER's first flyby, *Science*, *132*, 82–85.
- Arthur, C. W., R. L. McPherron, and J. D. Means (1976), A comparative study of three techniques for using the spectral matrix in wave analysis, *Radio Sci.*, *11*, 833–845.
- Boardsen, S. A., and J. A. Slavin (2007), Search for pick-up ion generated Na^+ cyclotron waves at Mercury, *Geophys. Res. Lett.*, *34*, L22106, doi:10.1029/2007GL031504.
- Glassmeier, K.-H., P. N. Mager, and D. Yu. Klimushkin (2003), Concerning ULF pulsations in Mercury's magnetosphere, *Geophys. Res. Lett.*, *30*(18), 1928, doi:10.1029/2003GL017175.
- Glassmeier, K.-H., D. Klimushkin, C. Othmer, and P. Mager (2004), ULF waves at Mercury: Earth, the giants, and their little brother compared, *Adv. Space Res.*, *33*, 1875–1883.
- Khrabrov, A. V., and B. U. O. Sonnerup (1998), Error estimates for minimum variance analysis, *J. Geophys. Res.*, *103*, 6641–6651.
- Kim, E.-H., and D.-H. Lee (2003), Resonant absorption of ULF waves near the ion cyclotron frequency: A simulation study, *Geophys. Res. Lett.*, *30*(24), 2240, doi:10.1029/2003GL017918.
- Kim, E.-H., J. R. Johnson, and D.-H. Lee (2008), Resonant absorption of ULF waves at Mercury's magnetosphere, *J. Geophys. Res.*, *113*, A11207, doi:10.1029/2008JA013310.
- Othmer, C., K.-H. Glassmeier, and R. Cramm (1999), Concerning field line resonances in Mercury's magnetosphere, *J. Geophys. Res.*, *104*, 10,369–10,378.
- Russell, C. T. (1989), ULF waves in the Mercury magnetosphere, *Geophys. Res. Lett.*, *16*, 1253–1256.
- Siscoe, G. L., N. F. Ness, and C. M. Yeates (1975), Substorms on Mercury?, *J. Geophys. Res.*, *80*, 4359–4363.
- Slavin, J. A., *et al.* (2008), Mercury's magnetosphere after MESSENGER's first flyby, *Science*, *132*, 85–89.
- Takahashi, K., R. L. McPherron, and W. J. Hughes (1984), Multispacecraft observations of the harmonic structure of Pc 3–4 magnetic pulsations, *J. Geophys. Res.*, *89*, 6758–6774.
- Zurbuchen, T. H., J. M. Raines, G. Gloeckler, S. M. Krimigis, J. A. Slavin, P. L. Koehn, R. M. Killen, A. L. Sprague, R. L. McNutt Jr., and S. C. Solomon (2008), MESSENGER observations of the composition of Mercury's ionized exosphere and plasma environment, *Science*, *132*, 90–92.
- M. H. Acuña, S. A. Boardsen, and J. A. Slavin, NASA Goddard Space Flight Center, Greenbelt, Mail Stop 674, MD 20771, USA. (scott.a.boarsen@nasa.gov)
- B. J. Anderson and H. Korth, Johns Hopkins University Applied Physics Laboratory, Laurel, MD 20723, USA.
- S. C. Solomon, Department of Terrestrial Magnetism, Carnegie Institution of Washington, 5241 Broad Branch Road, NW, Washington, DC 20015, USA.